BMC Oral Health

RESEARCH

Open Access

5'tiRNA-35-GlyTCC-3 and 5'tiRNA-33-CysGCA-11 target BMP6, CUL1 and SPR of non-syndromic cleft palate

Ruimin Liu[1,2†], Linxiang Zhang[1,2†], Peinan Hu[1,2†], Anni Liu[1,2], Yixin Zhang[3], Qian Liu[3], Jianqing Guo[4], Dong Han[5*], Haiquan Yue[2*] and Baoping Zhang[1*]

Abstract

Background tsRNAs are novel small non-coding RNAs that play important regulatory roles in gene expression, translation, transcription, and epigenetic modification through proteins or mRNAs and may be therapeutic targets for certain diseases. The etiology of non-syndromic cleft palate-only is complex and the pathogenesis is poorly understood, non-coding RNAs play important roles in its development.

Methods The tsRNAs of patients with simple cleft palate were compared with healthy individuals using small RNA microarray, bioinformatic analysis, quantitative real-time transcription polymerase chain reaction, and the effects measured using immunohistochemical staining.

Results Seventy-nine tsRNAs were upregulated and fifty-four tsRNAs were downregulated in patients with simple cleft palate compared with healthy individuals, among which the expression of 5'tiRNA-35-GlyTCC-3 and 5'tiRNA-33-CysGCA-11 was markedly different and was involved in key signaling pathways related to the development of the palate, such as the cell cycle, cAMP signaling pathway, BMP signal transduction, folate biosynthesis, and other key signaling pathways that determine anatomical structure occurrence, regulate gene expression during development, influence epigenetics, and other biological processes, its target genes include *BMP6*, *CUL1* and *SPR*.

Conclusion 5'tiRNA-35-GlyTCC-3 and 5'tiRNA-33-CysGCA-11 are closely associated with non-syndromic cleft palate development and are expected to be potential new targets for diagnosis and treatment.

Keywords tsRNA, Non-syndromic cleft palate, Microarray analysis, Enrichment analysis, RT-qPCR

†Ruimin Liu, Linxiang Zhang and Peinan Hu are co-first Authors.

*Correspondence:
Dong Han
59607654@qq.com
Haiquan Yue
yhq18693197645@163.com
Baoping Zhang
zhangbp@lzu.edu.cn

[1]School of Stomatology, Lanzhou University, Donggang West Road 199, Lanzhou 730000, China
[2]Department of Oral and Maxillofacial Surgery, Gansu Provincial Hospital, Lanzhou 730000, China
[3]The First Clinical Medical College, Gansu University of Chinese Medicine, Lanzhou 730000, China
[4]Department of Stomatology, Zhonghe 404 Hospital, Jiayuguan 735100, China
[5]Gansu Wuwei Tumor Hospital (Gansu Province Wuwei Academy of Medical Sciences), Wuwei 733000, China

Background

Nonsyndromic cleft lip with or without cleft palate (NSCL/P) is one of humans' most common congenital malformations. Orofacial clefts (OFC) can be anatomically divided into cleft lip and palate (CLP), cleft lip (CL), and cleft palate only (CP). Its etiology is complex and results from genetic and environmental factors [1–2]. In Asian populations, the incidence of cleft lip and palate varies among populations from different regions, with prevalence rates reaching as high as 1 in 500 newborns [3–4]. An epidemiological study conducted in Hunan province, China, revealed that among 847,755 infants born between 2016 and 2020, the incidence of CL/P was 0.81‰, while the incidence of CP was 0.30‰, with CP accounting for 36.79% of CL/P cases [5]. The incidence of the non-syndromic cleft palate only (NSCPO) subtype in China was 0.27 per 1,000 [6]. Furthermore, the latest meta-analysis established a link between environmental tobacco exposure (ETS) and the risk of nonsyndromic orofacial clefts (NSOFC), reporting a combined odds ratio of 1.80 based on factors such as phenotype, risk of bias, and year of publication [7]. A more in-depth look pointed out that maternal ETS exposure may be regulated by genetic susceptibility, including the variation of *TGFA*, *TGFB3*, and *MSX1* developmental genes. As well as the polymorphism of *CYP* (1A1, 2E1) and *GST* (M1, T1) family genes involved in the metabolic pathway of tobacco smoke compounds, studies have also observed a strong association between maternal smoking and *TGF-*ɑ gene variants in the risk of cleft lip [8–9]. Particularly for the childhood NSOFCs, such as the *IRF6* gene, which may influence CL/P risk in the Chinese population through interactions with multivitamin supplementation and ETS [10]. Etiologic studies suggest that the development of cleft lip and palate is related to genes, environment, drugs, immunity, and other factors, and it is a polygenic susceptibility disease influenced by the environment [11].

The most critical time for palatal development is from the 6th to the 9th week of the embryo. During the 6th week, the 2 lateral palatal processes or palatal shelves grow from the medial aspect of the maxillary protuberance and are located vertically positioned along with lateral side of the tongue [12]. When the tongue began to flatten and move downward due to mandibular development, the two palatal shelves began to rise to the horizontal position and approached each other. Subsequently, the palatal shelves fused with each other and fused with the nasal septum. The primary palatine process comes from the spherical process of the middle nasal process, and its occurrence is closely related to the development of the nasal plate, nasal concave, lateral nasal process, and maxillary process [13]. At the 6th week of the embryo, under the olfactory fossa, the bulbous process, in conjunction with the contralateral bulbous process and the maxillary process, continuously prolifers towards the oral side to form the anterior palatine process. The primary palatal process will form the premaxilla and maxillary incisors [14–15]. Eventually, fusion was completed in the 12th week. Bone fusion extending from the maxilla and palate to the palatal shelves formed the hard palate and the unossified part formed the soft palate and uvula [16]. Any factor during embryonic development that affects the palatine tissue contact and failure of fusion results in the appearance of a cleft [17]. Previous studies reported a new small RNA molecule as a novel epigenetic regulator that exerts biological roles through a miRNA-like approach [18]. There is increasing evidence that tsRNA has predictive value as a biomarker [19–21].

Transfer ribonucleic acid (tRNA) is an articulating molecule that decodes messenger RNA and translates proteins. Recent studies show that tRNAs are a major source of small non-coding RNAs (ncRNAs) with complex and diverse functions [22]. TsRNA is a small non-coding RNA derived from tRNA, approximately 14–30 nucleotides in length, divided into five subtypes based on biogenesis and length: tRF-5, tRF-3, tRF-2, tRF-1, and i-tRF [23]. TsRNA is involved in the occurrence and development of diseases through various mechanisms such as RNA silencing, regulatory translation, and RNA reverse transcriptional regulation, and has tissue-specific and expression stability [24]. In addition, the expression profile of tsRNAs shows dynamic changes during embryonic development, suggesting that it plays an important role in the maintenance of embryonic development [25]. Compared to miRNAs, tsRNAs are more conserved in *vivo* and better suited as biomarkers of disease [26–27]. TsRNAs have the potential to serve as prognostic and therapeutic biomarkers because of their close relationship to the emergence of several human diseases, including tumors, metabolic diseases, and intergenerational inheritance [28]. For example, sperm tsRNAs contribute to the intergenerational inheritance of acquired metabolic disorders [29], whereas tsRNAs are involved in mediating the regulation of intergenerational inheritance of metabolic disorders in high-fat diet-induced mice, and interventions with anti-inflammatory agents (5-ASA) reduce the expression level of Glu-CTC tsRNAs in spermatocytes which result in an improvement of glucose in female offspring tolerance, with a modest modulatory effect on the offspring phenotype [30]. Therefore, we hypothesize that tsRNAs are likely involved in epigenetic cleft lip and palate diseases, however, the tsRNAs involved in cleft lip and palate diseases are unreported.

This study focused on the regulatory role of tsRNAs in the nonsyndromic cleft palate. We explored the potential role of specific tsRNAs in NSCPO and the molecular mechanisms by small RNA microarray, quantitative

real-time polymerase chain reaction (RT-qPCR), bioinformatic analysis, and immunohistochemical methods to provide new ideas for the pathogenesis and diagnostic and therapeutic treatment of the nonsyndromic cleft palate.

Methods

Subject inclusion and experimental grouping

This study was approved by the Ethics Committee of Gansu Provincial People's Hospital (2022 – 363). Informed consent was obtained from each patient's family before sampling. Tissues on the cleft margin of the palate from patients diagnosed with NSCPO who attended the Department of Oral and Maxillofacial Surgery of Gansu Provincial People's Hospital between March 2022 and November 2023 were used as the experimental group. Normal palatal tissues adjacent to the cleft, sourced from the same NSCPO patients, constituted the control group. Inclusion criteria specified that individuals, apart from having NSCPO, should not have any other diseases, with ages ranging from 6 months to 60 months. The classification was based on the subtypes of cleft palate deformities outlined in the Classic International Classification of Cleft Deformities [31]. A small amount of healthy palatal tissue from healthy individuals with a clinical diagnosis of facial trauma, supernumerary tooth, etc., which were trimmed intraoperatively was received as a health group, and the age of the patients was less than 15 years old.

Clinical data characteristics

A preoperative questionnaire was used to collect general information and epidemiologic characteristics of the patients. Demographic data included sex, age, nationality, the presence of any common risk factors for NSCPO [32], and cleft palate deformity subphenotypes in the Classical International Classification.

Sample collection and processing

In this experiment, a total of 73 cases of NSCPO tissues (NSCPO group), 10 samples from the control group, and 71 samples of healthy tissues (health group) were included. Among them, 3 cases of NSCPO tissues (NSCPO group) and 3 cases of healthy tissues (health group) were used for small RNA microarray analysis, while 60 pairs of samples (NSCPO and health group) were used for RT-qPCR to detect the expression of key tsRNAs and target genes in the tissues, in order to validate the results of microarray sequencing. 8 healthy group samples, 10 control group samples, and 10 NSCPO tissue samples were used for subsequent immunohistochemical experiments to verify protein expression levels. After the tissue samples were first collected in a 1.5 ml sterile enzyme-free EP tube, the blood was first flushed with sterile PBS solution, then transferred to a enzyme-free frozen storage tube, and the tissue was immersed in RNA later solution at 4 ℃. After soaking overnight, the excess liquid in the tube was cleaned up, and the tissue was stored in a -80 °C refrigerator for future use. The above operations maintained a low-temperature environment throughout the ice operation.

RNA extraction

Tissue samples were removed from – 80 ℃ storage and immediately manipulated on ice. Total RNA was extracted using the M5 HiPer Universal RNA Mini Kit Tissue or Cellular Rapid RNA Extraction Kit Reagent (Mei5bio or polymerase), and the concentration and quality of the extracted RNA was assessed using the NanoDrop ND-1000 instrument (Thermo Fisher Scientific). RNA integrity was assessed using an Agilent 2100 Bioanalyzer analysis system.

Arraystar human small RNA array V1.0

Briefly, small RNA microarrays include RNA extraction, labeling, and array hybridization. For small RNA microarray profiling (Supplementary Table S1), the total RNA was firstly dephosphorylated and denatured by adding DMSO. The RNA end labeling was performed by adding ligase buffer, BSA, the final product 50 mM pCp-Cy3 and 15 units of T4 RNA ligase at 28 μL overnight reaction at 16 °C. 2× hybridization buffer (Agilent) was mixed with the completed labeling reaction to a final volume of 45 μL. The labeled sample was mixed on the microarray and hybridized at 55 °C for 20 h. The slides were washed at room temperature in 6× SSC containing 0.005% Triton X-100 for 10 min and then in 0.1× SSC containing 0.005% Triton X-100 for 5 min. The slides were scanned on the Agilent G2505C microarray scanner.

Data analysis

Agilent Feature Extraction software (version 11.0.1.1) was used to analyze the acquired array images. The raw intensities were log2 transformed and quantile normalized. After normalization, the probe signals having Present (P) or Marginal (M) QC flags in at least 3 out of 6 samples were retained. Multiple probes from the same small RNA (miRNA/tsRNA/pre-miRNA/tRNA/snoRNA) were averaged and consolidated into one RNA level. Differentially expressed small RNAs between two comparison groups were identified by filtering at the indicated fold change (FC) and statistical significance (p-value) thresholds. Hierarchical clustering, scatter plots, and volcano plots were generated by the R language limma package.

Gene Ontology (GO) analysis (http://geneontology.org/) provides the biological processes in which genes are involved, the location of cells, and their molecular functions. Pathway analysis was performed using the Kyoto

Encyclopedia of Genes and Genomes (KEGG) database (http://www.kegg.jp/). MiRNA can use its seed sequence (located at the 2–7 nt at the 5' end) to identify its mRNA target and inhibit the translation activity of the overall mRNA since many studies show that tsRNA acts similarly to miRNA. We used two algorithms of TargetScan and miRDB to predict the target mRNA of tsRNA respectively, and calculated all mRNAs of the two sets to ensure the comprehensiveness and accuracy of the prediction.

Quantitative RT-PCR validation

The top 13 tsRNA with differential expression folds from large to small and upregulated expression were listed to further verify the changes of tsRNA in NSCPO, and 6 tsRNAs were selected to verify their expression by RT-qPCR. The pretreated RNA precipitation was used to synthesize cDNA by the stem-loop method. We used GAPDH as an internal standard reference to detect the mRNA expression of its target genes by RT-qPCR. The primers of the differential tsRNAs and the primers of the target genes were provided by Guangzhou Ruibo Biotechnology Company.

Immunohistochemical method

Primary antibodies were employed in opposition to the subsequent proteins: BMP6 (M06924-1, Boster, China), SPR (bs-11784R, Bioss Antibodies, China) and CUL1 (K003246P, Solarbio, China). Briefly, tissues were fixed, dehydrated, embedded, and all staining was performed on each sample. Sections were incubated with primary antibodies, washed, and incubated with appropriate secondary antibodies (pv6000, Immunobridge, GBI). A light microscope (Olympus BX53) was used to image the stained sections. Semi-quantitative analysis was performed using Aipathwell v2 softwell (Servicebio, China).

Statistical analysis

The Student's t-test in SPSS software (v27.0, IBM, USA) was used to calculate the differences in the expression of tsRNA and mRNA between the NSCPO and health group, and when the relative expression of the target genes in the health group was set to 1, the $2^{-\Delta\Delta CT}$ value was the relative expression level of the target genes in the NSCPO group compared with that in the health group. The experimental data were continuous variable information, and the median was selected to distinguish the high and low expression of target genes and grouped. Clinical characteristics and tsRNA expression levels were analyzed by Chi-square test to calculate the odds ratio (OR) and 95% confidence interval (CI).

Results

Screening for differentially expressed tsRNAs

Human small RNA microarray analysis results showed that 350 tsRNAs were up-regulated while 250 tsRNAs were down-regulated in NSCPO tissues compared to the health group (Supplementary Table S2). 79 upregulated and 54 downregulated tsRNAs were detected by controlling the screening conditions to $p<0.05$,|log2 FC|>1.5 (Fig. 1). After sorting the differential expression multiples from large to small, we selected the top 13 upregulated tsRNA (Table 1).

GO and KEGG enrichment analyses were employed to predict the regulatory mechanisms of tsRNA-mRNA

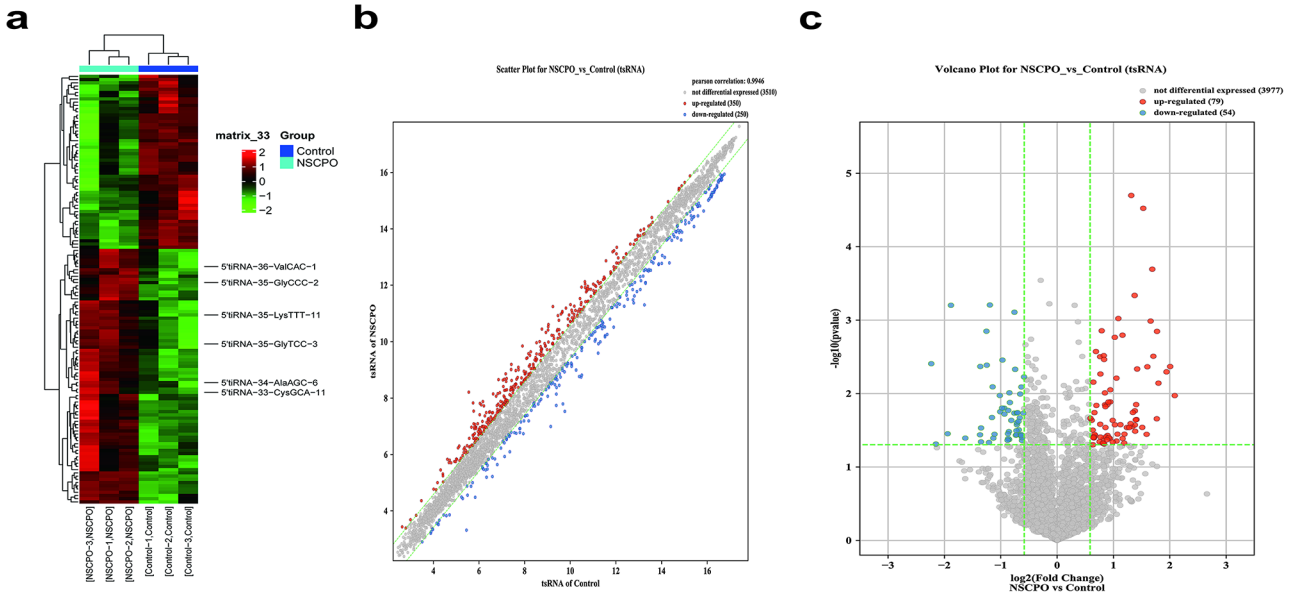

Fig. 1 Heatmap, scatter plot and volcano plot of differentially expressed tsRNAs in the NSCPO group compared with the Blank Ctrl group. (**a**) Heatmap of DE-tsRNAs. (**b**) Scatter plot of DE-tsRNAs. (**c**) Volcano plot of DE-tsRNAs

Table 1 Differential expression of DE-tsRNAs between Blank Ctrl and NSCPO groups

tsRNA-name	logFC	*P*-value	Change
5'tRF-ArgTCT	3.007	0.036	Up
5'tiRNA-MetCAT	2.631	0.023	Up
5'tRF-ArgTCG	2.602	0.017	Up
5'tRF-ArgCCG	2.259	0.029	Up
5'tiRNA-LeuCAA	2.101	0.036	Up
5'tiRNA-ValCAC	2.036	0.027	Up
5'tiRNA-CysGCA	1.819	0.039	Up
5'tiRNA-LysCTT	1.781	0.049	Up
5'tRF-TrpCCA	1.705	0.039	Up
5'tiRNA-GlyTCC	1.699	0.026	Up
5'tiRNA-AlaAGC	1.573	0.040	Up
5'tiRNA-GlyCCC	1.561	0.040	Up
5'tiRNA-LysTTT	1.506	0.022	Up

interactions. The results indicated that the top 13 significantly upregulated tsRNAs were primarily enriched in processes related to the morphogenetic regulation of dendritic spines, cell junctions, and burson biosynthesis. In contrast, the mRNAs targeted by these tsRNAs were mainly enriched in the folate biosynthesis pathway and the phospholipase D signaling pathway (Fig. 2; Table 2).

Among the top 13 upregulated tsRNA, RT-qPCR experiments were performed to validate microarray analysis results using clinical samples collected from 60 NSCPO cases and 60 health cases in total. The relative content of target genes was calculated according to the standard curve method and plotted using GraphPad Prism 9. The expressions of 5'tiRNA-34-AlaAGC-6, 5'tiRNA-36-ValCAC-1, 5'tiRNA-35-GlyTCC-3, 5'TiRNA-35-GlyCCC-2, 5'tiRNA-35-LysTTT-11, and 5'tiRNA-33-CysGCA-11 in the clinical samples of the experimental group were upregulated compared with the health group, which was consistent with the results of microarray analysis. The upregulation of 5'tiRNA-35-GlyTCC-3 and 5'tiRNA-33-CysGCA-11 was statistically significant (Fig. 3).

RNA secondary structure of 5'tiRNA-35-GlyTCC-3 and 5'tiRNA-33-CysGCA-11 by Forna visualization

The 5'tiRNA-35-GlyTCC-3 and 5'tiRNA-33-CysGCA-11 secondary structures were visualized using forna [33]. Forna provides a suitable platform for the conversion of static text representation to 2D images. The proteins were represented as larger grey nodes, with dashed lines denoting interactions between the various strands. The initial position of each node, or nucleotide, was determined using the NAView algorithm [34], but was subsequently optimized by force oriented layout algorithm was optimized to obtain the tsRNA secondary structure map, Fig. 4. TsRNAs can be used by pairing with the mRNA 3'-UTR, and there have reported that the 3' terminus of a small RNA derived from Leu-CAG tRNA (LeuCAG 3'tsRNA) regulates the human tRNA by maintaining the ribosomal protein S28 (RPS28) levels to regulate ribosomal biosynthesis in humans. By binding to two target sites in the RPS28 mRNA and disrupting the secondary structure of the two target sites: the coding sequence (CDS) and the 3'UTR of the two targets [35], it was predicted that 5'tiRNA-35-GlyTCC-3 and 5'tiRNA-33-CysGCA-11 may interact with the target genes in the same manner.

Protein-protein interaction (PPI) network construction to visualize differentially expressed tsRNA and genes

Constructing and visualizing the PPI networks of target genes using the Search Tool for Interacting genes (STRING) web site (http://string-db.org) and Cytoscape, the structure of PPI network and the weighted

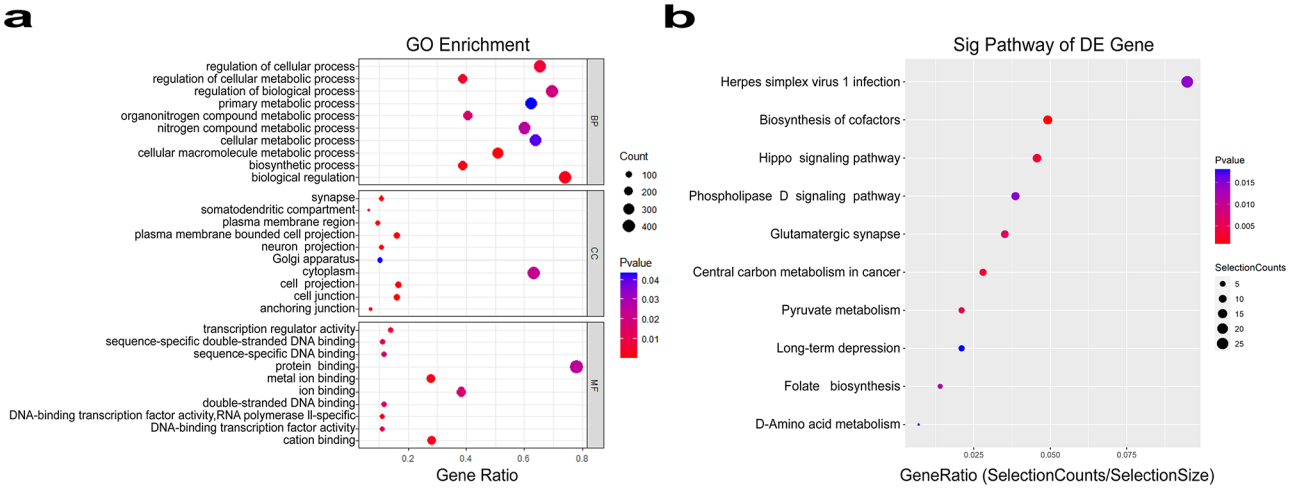

Fig. 2 Functional enrichment of analysis of the top 13 up-regulated tsRNAs based on GO and KEGG. (**a**) The top 10 terms in the GO category of GO analyses the top 13 up-regulated tsRNAs. (**b**) The top 10 KEGG pathways analysis of the top 13 up-regulated tsRNAs

Table 2 The top 10 KEGG pathways enriched by the target genes corresponding to the top 13 up-regulated tsRNAs

Pathway ID	Name	Count	*P*-value	Genes
hsa05168	Herpes simplex virus 1 infection	495	0.0143	HLA-DQA2//PPP1CC//SRPK1//TAPBP//ZNF107//ZNF208//ZNF224//ZNF267//ZNF275//ZNF316//ZNF354C//ZNF417//ZNF44//ZNF441//ZNF460//ZNF468//ZNF471//ZNF510//ZNF543//ZNF558//ZNF566//ZNF583//ZNF614//ZNF773//ZNF780A//ZNF84//ZNF853
hsa01240	Biosynthesis of cofactors	153	0.001	AKR1A1//BCAT1//BCO1//DHFR//GCH1//GGCX//IDO2//KYNU//MOCS2//NMNAT1//RDH11//SPR//UGDH//UGT2B7
hsa04390	Hippo signaling pathway	157	0.003	BMP6//BMPR1A//CCND1//DLG3//DVL3//FRMD1//MYC//PATJ//PPP1CC//TEAD1//TGFBR1//WNT4//YWHAZ
hsa04072	Phospholipase D signaling pathway	148	0.015	AVPR1B//DGKQ//GNAS//GRM5//KIT//KITLG//LPAR3//PDGFA//PIK3R5//PIP5K1A//PLA2G4E
hsa04724	Glutamatergic synapse	114	0.0065	GLS//GLS2//GNAI1//GNAQ//GNAS//GRK3//GRM5//ITPR2//PLA2G4E//SLC17A8
hsa00470	D-Amino acid metabolism	6	0.017	GLS//GLS2
hsa05230	Central carbon metabolism in cancer	70	0.0029	GLS//GLS2//HK1//KIT//MYC//PDHA1//PDHA2//PDHB
hsa04110	Cell cycle	126	0.033	CCND1//GADD45B//MDM2//MYC//ORC2//ORC3//ORC4//RBX1//YWHAZ
hsa04066	HIF-1 signaling pathway	109	0.037	ENO1//HK1//IGF1R//PDHA1//PDHA2//PDHB//RBX1//TLR4
hsa03060	Protein export	23	0.045	SEC61B//SPCS1//SRP72

connections between nodes were screened for Hub genes by maximum clique centrality (MCC) (Fig. 5).

Target gene loci for differential tsRNA in NSCPO tissues

Three target genes in 5'tiRNA-35-GlyTCC-3 and 5'tiRNA-33-CysGCA-11 were selected for subsequent validation. *CUL1* and *BMP6* were the target genes of 5'tiRNA-35-GlyTCC-3, and *SPR* was the target of 5'tiRNA-33-CysGCA-11 genes and key features of the two tsRNA binding sites (such as seed sequence and 3' end pairing information) were illustrated by miRanda and TargetScan (Fig. 6 and See Fig. 7).

Bioinformatic analysis of 5'tiRNA-35-GlyTCC-3 and 5'tiRNA-33-CysGCA-11

We performed GO and KEGG analysis on the two tsRNA and their target genes to further study the specific functions of non-syndromic cleft palate and 5'tiRNA-35-GlyTCC-3, 5'tiRNA-33-CysGCA-11. The top 10 pathways enriched by GO, include multiple processes. For example, 5'tiRNA-35-GlyTCC-3 is related to chemical homeostasis (GO: 0048878), developmental process (GO: 0032502), multicellular organism development (GO: 0007275), anatomical structure development (GO: 0048856), cellular response to endogenous stimulus (GO: 0071495) and other processes (Fig. 7). The 5'tiRNA-33-CysGCA-11 is related to the regulation of sodium ion transmembrane transport (GO: 1902305), the regulation of gene expression, epigenetics (GO: 0040029), and other processes (Fig. 8) (Supplementary Table S3-6).

Clinical information collection and analysis

Based on the international standard of cleft palate phenotype, the patients were categorized into three types, namely I, II, and III [36–37]. Subsequently, an analysis was conducted to investigate the relationship between tsRNA expression and the clinicopathological features of the patients (Table 3). Based on the relative expression levels of 5'tiRNA-35-GlyTCC-3 and 5'tiRNA-33-CysGCA-11, the patients were divided into two groups, those below the median were considered as the low expression group, and those above the median were considered as the high expression group, and the number of people in the two groups were counted for the chi-square test. The patient cohort comprised 27 boys and 33 girls, ranging in age from 6 to 60 months, with an average age of 14 ± 15 months. No significant correlation was observed between the expression of the 5'tiRNA-35-GlyTCC-3 and sex, classification, age, folic acid supplementation during pregnancy, toxic exposure, medication, and other characteristics ($p > 0.05$). In contrast, the relative expression of the 5'tiRNA-33-CysGCA-11 demonstrated a significant association with folic acid supplementation during pregnancy ($p < 0.05$). Among the patients, 18 were of Han nationality, while 42 belonged to various ethnic minorities (such as Hui, Tibetan, and Dongxiang, etc.). Additionally, 21 patients had a genetic history in their family, whereas 39 patients had no such history. The relative expression levels of the 5'tiRNA-35-GlyTCC-3 and 5'tiRNA-33-CysGCA-11 exhibited significant statistical differences when compared to common risk factors, including nationality, genetic history, smoking,

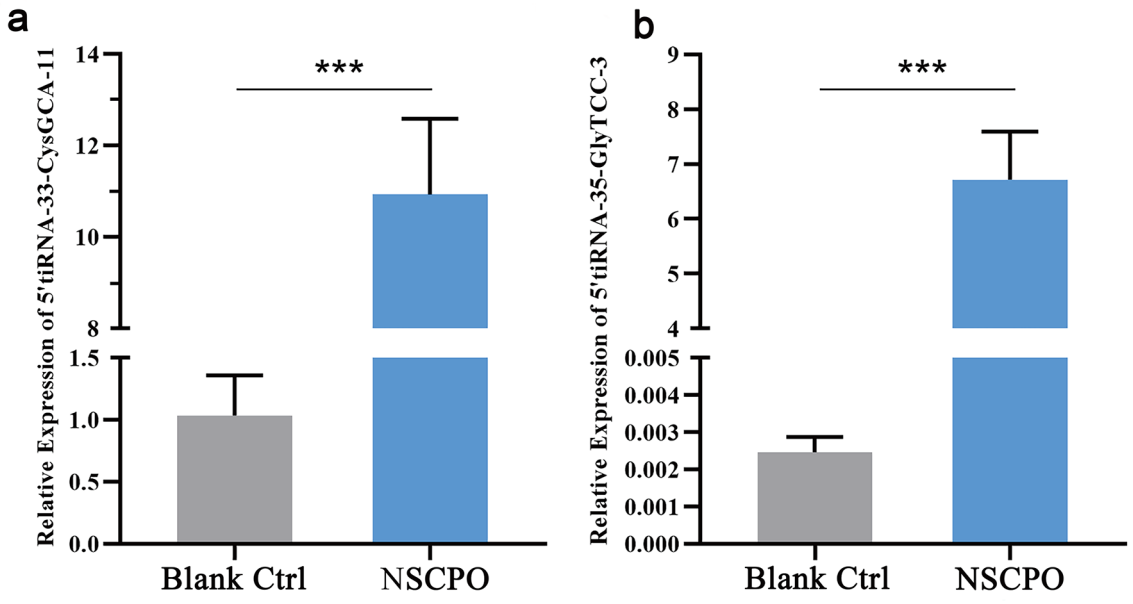

Fig. 3 Relative expression of two key tsRNAs 5'tiRNA-33-CysGCA-11 (**a**) and 5'tiRNA-35-GlyTCC-3 (**b**) in clinical samples by RT-PCR. (***$p < 0.001$)

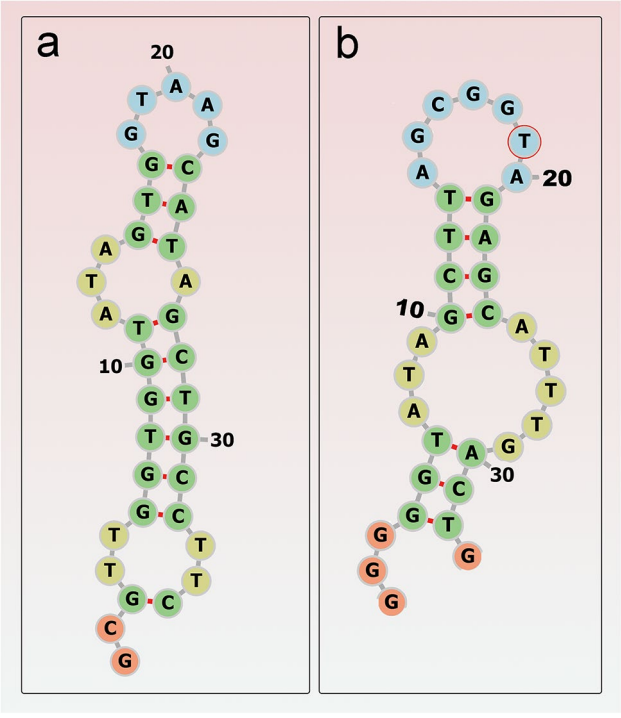

Fig. 4 Secondary structure of two key tsRNAs. (**a**) 5'tiRNA-35-GlyTCC-3. (**b**) 5'tiRNA-33-CysGCA-11

and drinking habits ($p < 0.05$). Furthermore, when the childbearing age was within the 25–29 age group, significant statistical differences were observed in the relative expression levels of the 5'tiRNA-35-GlyTCC-3 and 5'tiRNA-33-CysGCA-11, in comparison to parents' reproductive age falling below 19 or exceeding 30 ($p < 0.05$).

BMP6, CUL1, SPR downregulation confirmation by quantitative RT-PCR

In 60 pairs of tissues, *BMP6*, *CUL1*, and *SPR* were downregulated by at least 3-fold in NSCPO compared with health tissues ($p < 0.001$, Fig. 9).

Immunological observation of BMP6, CUL1, and SPR in NSCPO tissues

As shown in Fig. 10, for the BMP6 protein expression, the positive expression area (PEA) ratio of the health group was 3.29 ± 0.19, indicating a higher expression level of BMP6 protein in normal tissues. In contrast, the PEA ratio in the control group was significantly reduced to 0.57 ± 0.41, while the ratio of PEA in the NSCPO group was 2.16 ± 0.29, lower than the health group but higher than the control group. Statistical analysis showed that the area of positive expression of BMP6 was reduced by more than half in the NSCPO group compared to the health group ($p < 0.05$), while the expression level of BMP6 was widespread and significant in normal tissues ($p < 0.001$). These results indicate low expression levels of BMP6 in the epithelial region and connective tissue of the NSCPO group. The PEA ratio of CUL1 was 4.98 ± 0.41 in the health group, and 2.63 ± 0.23 in the NSCPO group was similar to 2.46 ± 0.21 in the control group. The PEA ratio of SPR was 7.83 ± 1.61 in health group and 1.44 ± 0.13 in control group, which was higher than 2.16 ± 0.29 in NSCPO group. The results showed that CUL1 and SPR were widely expressed in normal tissues ($p < 0.001$), however, there was no significant difference in expression level between NSCPO group and control group ($p > 0.05$). Aipathwell v2 was used to

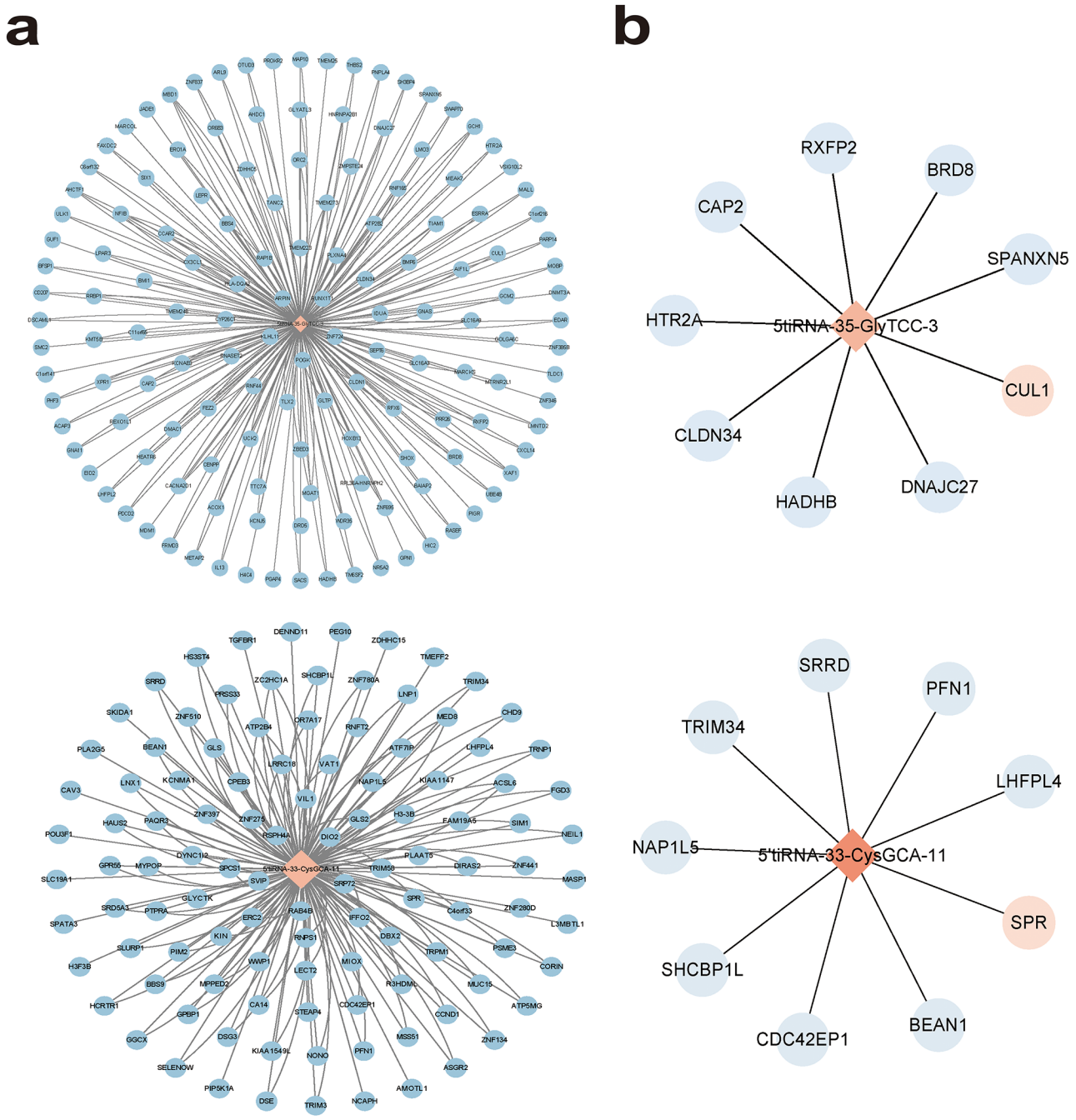

Fig. 5 Protein-protein interaction network complex. (**a**) The protein-protein interaction network visualized by Cytoscape. (**b**) The top 10 hub genes calculated by MCC algorithm in PPI network

semi-quantitatively analyze and calculate the positive area ratio. The expression trend of each group was basically consistent with the RT-qPCR results.

Discussion

NSCL/P is one of the most prevalent forms of NSOFC. This congenital dysmorphic genetic disorder arises from a complex interplay of multiple factors, including both genetic and non-genetic influences, as well as gene-gene and gene-environment interactions. Previous studies have shown that the folic acid can affect the phosphorylation of STAT3 signaling and further regulate JAK2/STAT3 pathway, removes p63 and K17 positive epithelial seams [38], which involved in the development of cleft palate. But p63 is involved in the development of the oral epidermis to prevent premature and pathological epithelial adhesion in early embryology [39] and its mutations can cause cleft palate in humans and mice and certain

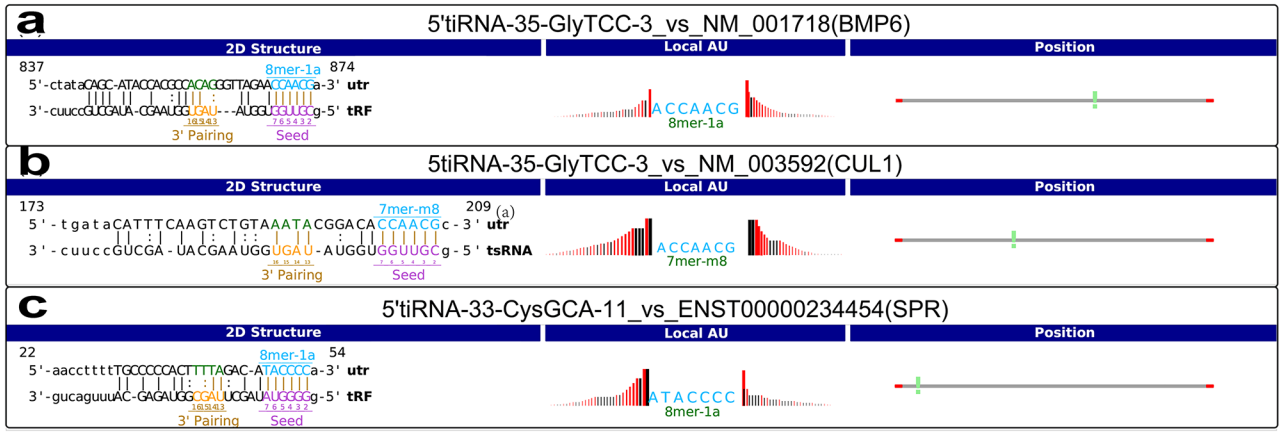

Fig. 6 Target three key gene loci of two key tsRNAs in NSCPO tissues. (**a**) 5'tiRNA-35-GlyTCC-3 targets BMP6. (**b**) 5'tiRNA-35-GlyTCC-3 targets CUL1. (**c**) 5'tiRNA-33-CysGCA-11 targets SPR

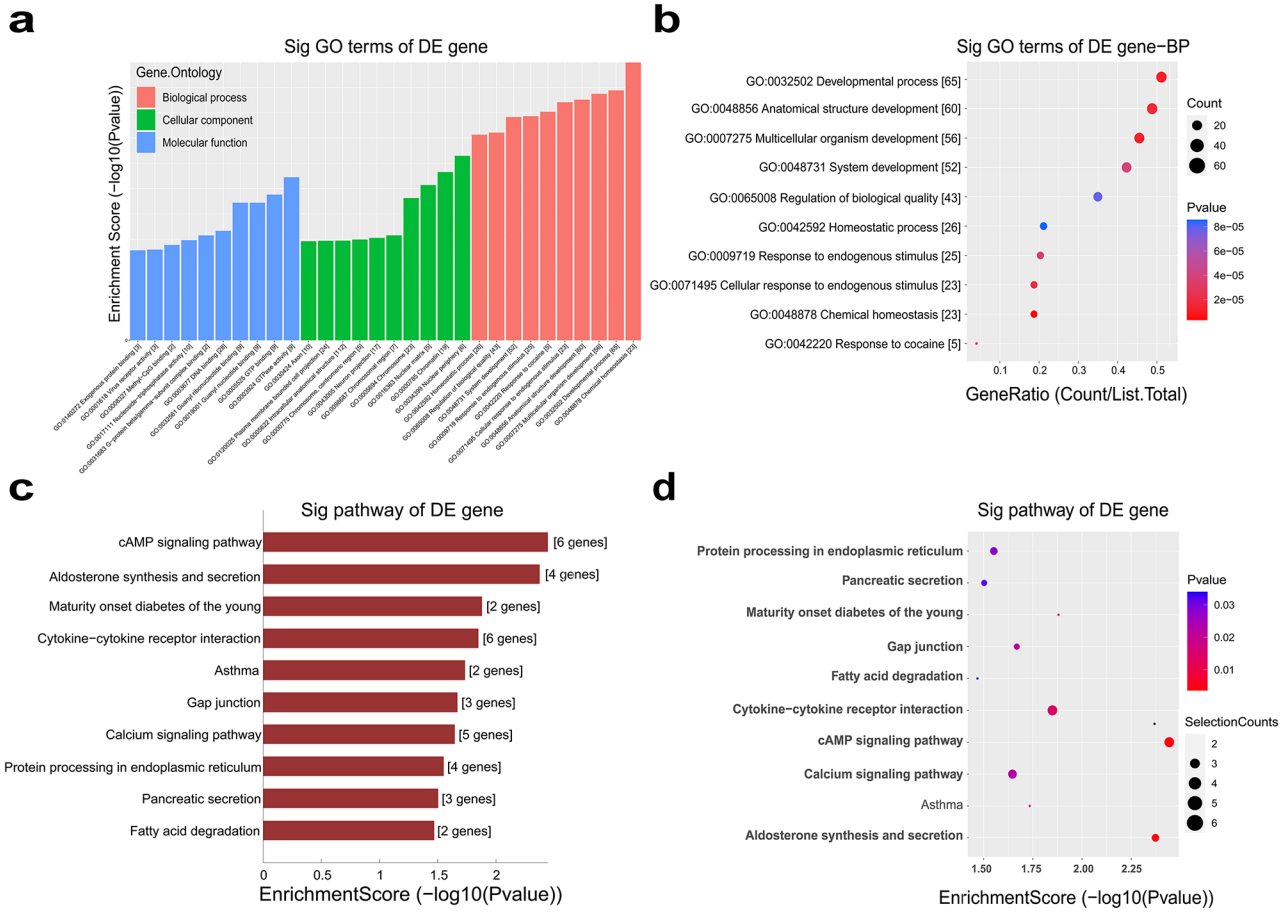

Fig. 7 Functional enrichment of analysis of the 5'tiRNA-35-GlyTCC-3 based on GO and KEGG. **a**-**b**. The top 10 terms in the GO category of GO analyses the 5'tiRNA-35-GlyTCC-3. **c**-**d**. The top 10 KEGG pathways analysis of the 5'tiRNA-35-GlyTCC-3

external factors such as folic acid supplementation can affect certain signaling pathways, thereby sparing the development of cleft palate. In addition, while BMP6 can regulate the proliferation and differentiation of cells by affecting the expression of JAK2 gene [40]. It is suggested that BMP6 could affect palate development through JAK2/STAT3 signaling pathway. Due to the expression profile of tsRNAs plays an important role in the maintenance of embryonic development, in this study, we found that the expression of 5'tiRNA-35-GlyTCC-3

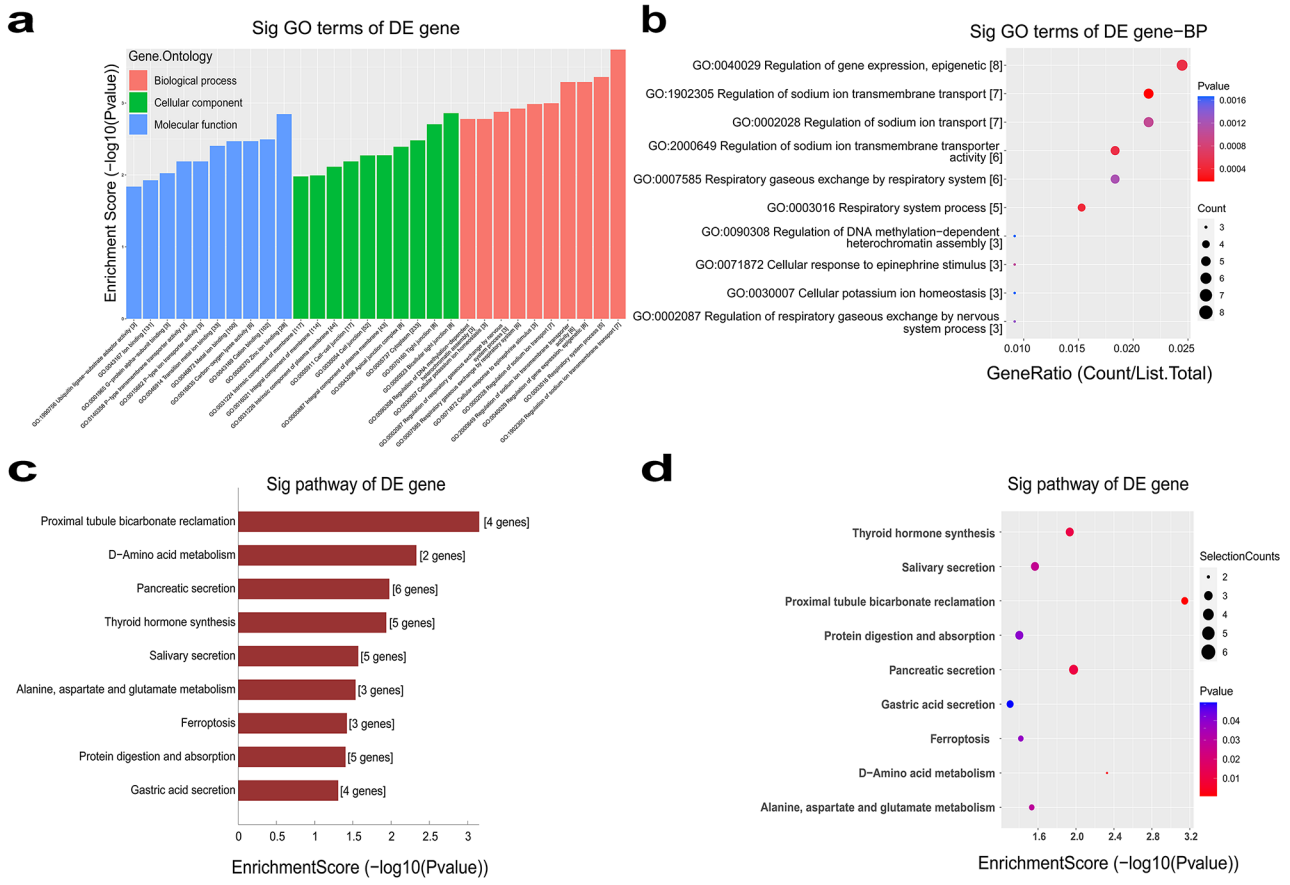

Fig. 8 Functional enrichment of analysis of the 5'tiRNA-33-CysGCA-11 based on GO and KEGG. **a**-**b**. The top 10 terms in the GO category of GO analyses the 5'tiRNA-33-CysGCA-11. **c**-**d**. The top 10 KEGG pathways analysis of the 5'tiRNA-33-CysGCA-11

and 5'tiRNA-33-CysGCA-11 in NSCPO tissues was significantly upregulated, thus we infer that the targeted tsRNAs may influence the STAT3 signaling pathway involved in the cleft palate process by targeting the expression of BMP6.

TsRNA are a new class of ncRNAs that have begun to attract our attention owing to their role in gene silencing, ribosome biogenesis, reverse transcription translocation, and epigenetic inheritance, as well as their involvement in the regulation of a variety of human diseases such as neurological disorders, metabolic disorders, and cancer. In recent years, small RNA microarrays have enabled the systematic study of tRNAs, which are classical ncRNAs. Normally, tRNAs are spliced into a series of small molecule nucleic acid fragments that are tRFs and tiRNAs, collectively referred to as tsRNAs under conditions of sex hormones, hypoxia, and other stressful stresses. In normal cells, tRFs act as endogenous apoptotic signals to inhibit the regulators of relevant apoptotic proteins and cause apoptosis, either directly or indirectly. When cells are stressed, tRF is significantly increased, leading to an escape from regulation of the apoptotic process while inducing tumor cell proliferation. In lung cancer, tRF Leu-CAG interacts with AURKA proteins and regulates the Wnt/β-catenin and PI3K/AKT signaling pathways to alter histones to induce epithelial-to-mesenchymal transition [41]. Most of the literature reports that tsRNAs play regulatory roles in a miRNA-like manner, and some tRFs and miRNAs have similar functions in inhibiting mRNA translation. For example, 3-tRFs derived from tRNALeu-CAG in non-small-cell lung cancer (NSCLC) cells have similar roles to miRNAs to attenuate the translation of proteins [42]. tRFs act as miRNAs in *Drosophila melanogaster*. The 5'-and 3'-ends of *Drosophila* tRFs contain seed regions that preferentially match the conserved regions of 3'-untranslated regions (3'-utr), exons, and introns in the 12 *Drosophila* genomes. tRF-5 and tRF-3 have typical seed regions and can form tRF-miRNA chimeras [43]. This suggests that tsRNA plays a role in the mechanism of NSCPO. Our results identified two differentially expressed tsRNA of 5'tiRNA-35-GlyTCC-3 and 5'tiRNA-33-CysGCA-11 according to its larger fold change, smaller *p*-value, and RT-qPCR verification from human NSCPO patient samples. There are no reports on the role of tsRNA in the NSCPO phenotype.

Table 3 Correlation between the relative expression of 5'tiRNA-35-GlyTCC-3 and 5'tiRNA-33-CysGCA-11 with clinical pathologic features

Features	Classification	Total(*n*)	5'tiRNA-35-GlyTCC-3				5'tiRNA-33-CysGCA-11			
			High(*n*)	Low (*n*)	*P* value	OR (95%CI)	High (*n*)	Low (*n*)	*P* value	OR (95%CI)
Sum	60	60	42	18			45	15		
NSOFC subtype	I+II	24	15	9	0.301	0.556 (0.181-1.701)	18	6	1.000	1.000(0.303-3.296)
	III	36	27	9			27	9		
Sex	Male	27	21	6	0.234	2.000 (0.632-14.699)	21	6	0.653	1.313(0.400-4.303)
	Female	33	21	12			24	9		
Age	6–24 m	30	18	12	0.091	0.375 (0.118-1.190)	18	9	0.178	0.444(0.135-1.465)
	24–60 m	30	24	6			27	6		
Nationality	The Han nationality	18	6	12	<0.001***	0.083 (0.023-0.308)	6	12	<0.001***	0.038(0.008-0.178)
	Minority nationality	42	36	6			39	3		
Home address	Rural area	39	36	3	<0.001***	30.000 (6.620-135.956)	36	3	<0.001***	16.000(3.713-68.955)
	Cities and towns	21	6	15			9	12		
Folic acid supplementation during pregnancy	Yes	33	24	9	0.610	1.333 (0.440-4.037)	12	12	0.035*	0.091(0.008-1.077)
	No	27	18	9			33	3		
Exposure of indirect toxic substances during pregnancy	Yes	3	3	0	0.245	0.684 (0.574-0.816)	3	0	0.305	0.737 (0.631-0.861)
	No	57	39	18			42	15		
Take medication by mistake in early pregnancy	Yes	6	3	3	0.260	0.385(0.070-2.121)	6	0	0.136	0.722 (0.612-0.852)
	No	54	39	15			39	15		
Passive / active maternal smoking during pregnancy	Yes	15	3	12	<0.001***	0.038(0.008-0.178)	3	12	<0.001***	0.018(0.003-0.100)
	No	45	39	6			42	3		
Drinking during pregnancy	Yes	18	6	12	<0.001***	0.083(0.023-0.308)	6	12	<0.001***	0.038(0.008-0.178)
	No	42	36	6			39	3		
Family genetic history	Yes	21	21	0	<0.001***	0.538 (0.403-0.720)	24	0	<0.001***	0.583(0.443-0.769)
	No	39	21	18			21	15		
Average age of the parents	≤19	15	9	6	0.206[a]	3.000(0.533-16.897)	15	0	<0.001[a]***	0.333(0.132-0.840)
	20-24	6	3	3	0.519[b]	2.000(0.241-16.612)	3	3	0.519[b]	2.000(0.241-16.612)
	25-29	9	3	6	<0.001[c]***	18.00(2.892-112.044)	3	6	0.008[c]**	8.000(1.537-41.637)
	≥30	30	27	3			24	6		

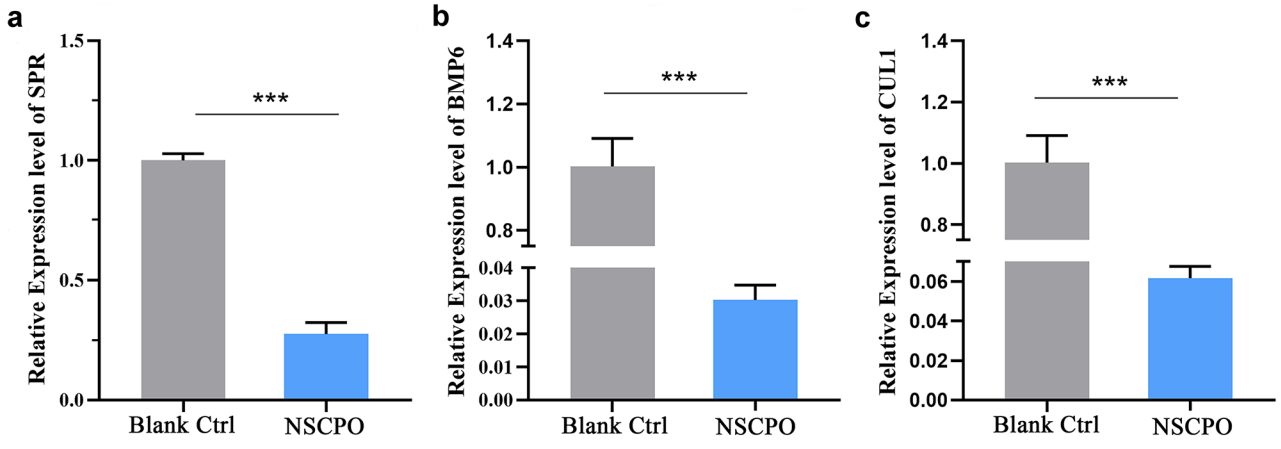

Fig. 9 Relative expression of three key mRNAs SPR (**a**), BMP6 (**b**) and CUL1 (**c**) in clinical samples by RT-qPCR. (**** $p < 0.0001$; *** $p < 0.001$; ** $p < 0.01$)

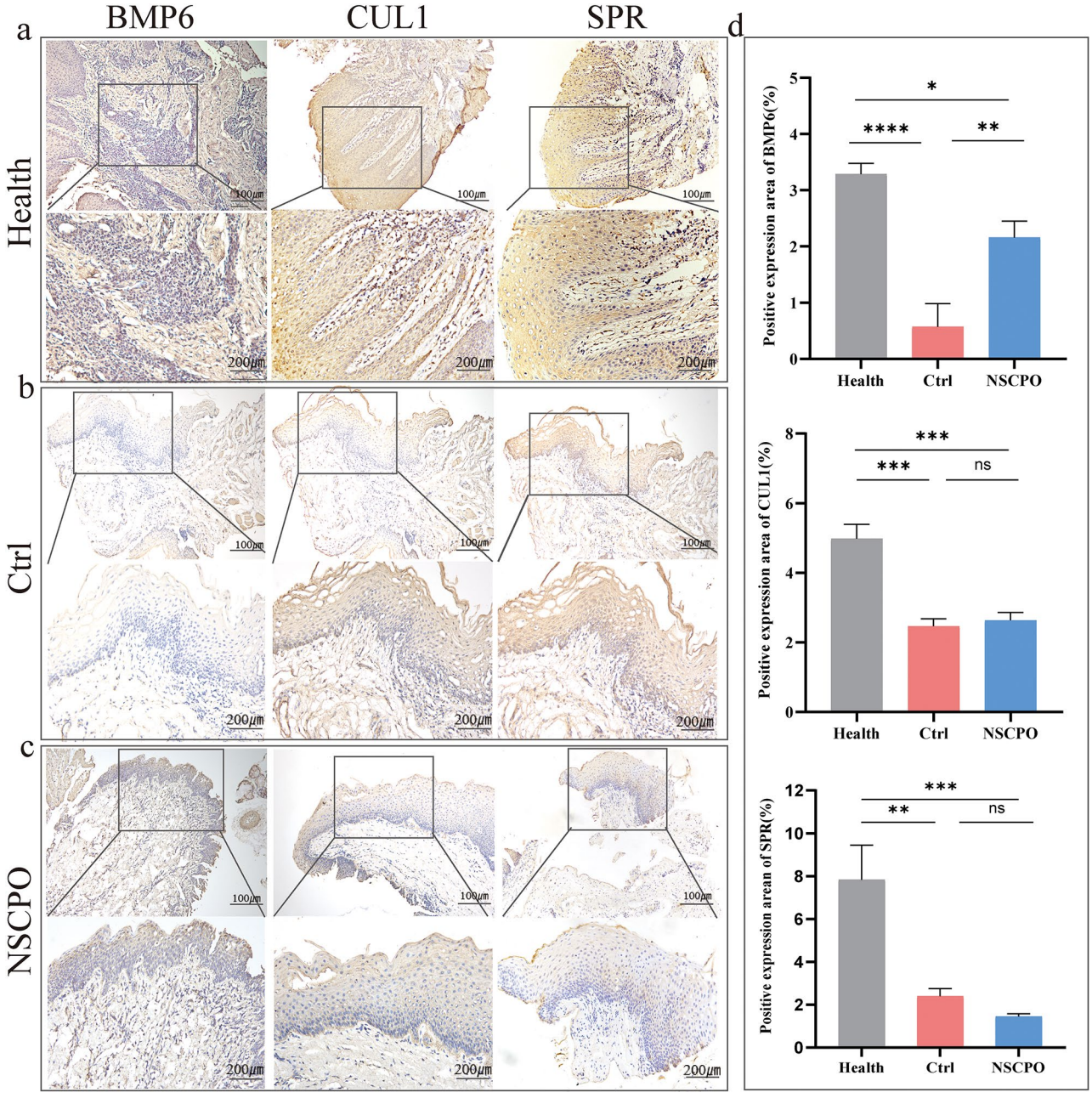

Fig. 10 Immunohistochemistry staining of BMP6, CUL1, SPR in the Health, Ctrl and NSCPO tissue

The development of cleft palate involves a series of processes such as cell proliferation, migration, osteogenesis and epithelial mesenchymal transformation. Once these processes are disrupted, they may lead to cleft palate. Folate metabolism is considered to be the basis of cleft lip and palate development, and genetic variation involved in folate metabolism may regulate maternal susceptibility to offspring with non-syndromic cleft lip and palate [44–45]. Tetrahydrofolate is the active form of folate, which works in the body. It is reduced from dihydrofolate, a product of thymidylate synthase reaction, under the catalysis of dihydrofolate reductase (DHFR) 3. DHFR can also catalyze the reduction of dihydrobiopterin (BH2) to tetrahydrobiopterin (BH4). Some studies suggest that folic acid metabolism disorder may be due to excessive BH2 inhibiting DHFR activity, so dynamic changes of DHFR and BH2 will affect folic acid metabolism [46–47]. SPR is an important regulatory factor for BH4 biosynthesis, which plays a certain role in maintaining the level of intracellular BH4. In addition, the bioavailability and oxidation status of biopterin appear to directly or indirectly influence various physiological processes, including the

metabolic pathways of folate. SPR may indirectly participate in folic acid metabolism through the interaction between BH4 and BH2 and DHFR [48–49]. GO and KEGG enrichment analysis showed that CUL1 acts as a protein-folding catalyst and molecular chaperone in the protein processing of endoplasmic reticulum. In addition, CUL1 is involved in the Wnt signaling pathway and TGF-β signaling pathway. Cullin-RING ubiquitin ligase (CRL), also known as SCF, and several CRL1 complexes, including $CRL1^{SKP2}$, $CRL1^{FBXO4}$, $CRL1^{FBXW8}$, $CRL1^{FBXO25}$ and $CRL1^{FBXO31}$, target cyclin D. After entering the S phase, cyclin D is phosphorylated by glycogen synthase kinase 3β (GSK3β) on threonine 286 (Thr286), triggering the interaction between cyclin D and CRL1 substrate receptors [50]. CUL1 protein acts as a scaffold protein in the Skp1-CUL1-Fbox (SCF) E3 ligase complex and regulates early embryonic development. Cyclin E is a physiological substrate of SCF E3 [51–52]. The SCF complex binds to one of approximately 70 F-box proteins that bind to specific substrates through SKP1 and regulates a variety of biological processes, including cell cycle regulation, cell growth, cell death, development, and differentiation [53–54]. BMP6 is a bone morphogenetic protein 6, and a member of the 60 A subfamily of the BMP family. This gene encodes a secretory ligand of the TGF-β (transforming growth factor-β) protein superfamily. *BMP2* and *BMP4* mRNA are expressed in the facial primordia of chicken and mammalian embryos in a dynamic pattern. BMP4 expression is restricted to distal epithelial cells of the medial nasal eminence, lateral nasal eminence, maxillary eminence, and mandibular eminence. The BMP signaling pathway regulates cellular value-addition, cellular differentiation, and apoptosis, which are critical steps in facial morphogenesis [55]. We verified the downregulation of *BMP6*, *CUL1*, and *SPR* in NSCPO tissues by RT-qPCR. 5'tiRNA-35-GlyTCC-3 plays a definite regulatory role in NSCPO disease by targeting *CUL1* and *BMP6* genes, and 5'tiRNA-33-CysGCA-11 by targeting the *SPR* gene. The BMP6 protein is involved in the epithelial-mesenchymal transition (EMT) phenotype, cell growth, and proliferation [56]. SPR can be converted into BH2 from the exogenous precursor vesicular protein, and BH4 can be regenerated from its oxidized form BH2 in a process catalyzed by the rate-limiting salvage enzyme, dihydrofolate reductase (DHFR). Skp1-CUL1-Fbox (SCF) E3 regulates cell cycle, proliferation, development, and other physiological processes by acting on three F-box proteins: β-TRCP, SKP2, and FBXW7 [57]. In summary, these reports provide strong evidence for our research.

GO enrichment analysis was used to further characterize the regulatory functions of these tsRNAs in NSOFC. These tsRNAs were enriched in many pathways, and these biological process abnormalities may play a role in the abnormal development of NSCPO's maxillofacial region. GO analysis of 5'tiRNA-35-GlyTCC-3 suggested that chemical homeostasis, development of anatomical structure, development process, and cell response to endogenous stimuli would affect the occurrence and development of NSCPO. At the same time, GO analysis of 5'tiRNA-33-CysGCA-11 suggested that the regulation of sodium ion transmembrane transport and the regulation of gene expression affected the occurrence and development of NSCPO.

However, this study has several limitations. The sample we used for microarray analysis was relatively small, and there may be differences in microarray analyses that were not based on cleavage fractionation. The clinical validation samples were all from northwest China, and the ethnic minorities were mostly Tibetan and Hui. There may be individual or regional differences in the experiment. Future research will focus on the biological functions and interactions between tsRNA and mRNA. No relevant cell or animal model was established to further verify the regulatory relationship determined from the molecular and target gene regulatory networks owing to the limited sample size. Subsequently, in vitro cell experiments can be used to verify the development process that the target gene may affect by knocking down the target tsRNA, combined with molecular biology such as CCK-8, scratch test, and Alizarin red staining.

Conclusion

In summary, we found that 5'tiRNA-35-GlyTCC-3 and 5'tiRNA-33-CysGCA-11 were upregulated in patients with NSCPO. The expression levels of the two tsRNA were related to the patient's nationality, family genetic history, and common risk factors such as smoking and drinking. Folic acid supplementation during pregnancy mainly affects the expression level of 5'tiRNA-33-CysGCA-11, and there is no statistical difference in the relative expression of the two tsRNA when parents are older than 19 years old or younger than 30 years old. Through the construction and functional analysis of 5'tiRNA-35-GlyTCC-3 and 5'tiRNA-33-CysGCA-11 related regulatory networks, we found that tsRNA and their target genes may play a crucial role in the etiology of NSCPO. It is expected that our study will provide some new clues for the preliminary understanding of the regulatory mechanism of tsRNA in NSCPO and provide new targets for the potential diagnosis and treatment of the non-syndromic cleft palate. In terms of biomarkers, the changes in the expression of 5'tiRNA-35-GlyTCC-3 and 5'tiRNA-33-CysGCA-11 can be preliminarily screened for high-risk patients with NSCPO. tsRNA can be detected in the blood, which greatly facilitates the early diagnosis and prevention of NSCPO. And the expression level of tsRNA may be related to the severity of NSCPO typing. The more severe the cleft palate, the higher the relative

expression level of tsRNA. In terms of therapeutic targets, follow-up studies can explore changes in the progression of NSCPO through overexpression or knockout of its coding genes. However, the structure of tsRNA is complex and diverse, and further exploration is needed to study the diagnosis and treatment of NSCPO, and there is also a lack of effective methods to regulate tsRNA expression.

Supplementary Information

The online version contains supplementary material available at https://doi.org/10.1186/s12903-025-05661-8.

Supplementary Material 1

Supplementary Material 2

Supplementary Material 3

Supplementary Material 4

Supplementary Material 5

Supplementary Material 6

Supplementary Material 7

Supplementary Material 8

Supplementary Material 9

Supplementary Material 10

Supplementary Material 11

Supplementary Material 12

Acknowledgements

We would like to thank the participants who agreed to participate in this study.

Author contributions

Ruimin Liu: Data curation, Writing-original draft. Linxiang Zhang: Writing-original draft, Data curation. Peinan Hu: Data curation, Charting. Yixin Zhang: Validation. Anni Liu: Validation. Qian Liu: Validation. Jianqing Guo: Supervision. Dong Han: Validation. Haiquan Yue: Validation. Baoping Zhang: Project administration, Conceptualization, Writing-review and editing, Validation.

Funding

The work was supported by the National Natural Science Foundation of Gansu Province (23JRRA1080); Natural Science Foundation of Gansu Province (23JRRA1289); Internal Fund of Gansu Provincial People's Hospital (ZX-62000001-2022-259); Fundamental Research Funds for the scientific research fund of School (Hospital) of Stomatology Lanzhou University ((22)0660; lzukqky-2022-t12; lzukqky-2022-t16); Internal Fund of Gansu Provincial People's Hospital (22GSSYD-44).

Data availability

All data generated or analysed during this study are included in this published article and its supplementary information files.

Declarations

Ethics approval and consent to participate

This study was approved by the Ethics Committee of Gansu Provincial People's Hospital (2022 – 363).

Consent for publication

Not applicable.

Competing interests

The authors declare no competing interests.

Received: 28 March 2024 / Accepted: 13 February 2025
Published online: 26 February 2025

References

1. Yoshioka H, Li A, Suzuki A, Ramakrishnan SS, Zhao Z, Iwata J. Identification of microRNAs and gene regulatory networks in cleft lip common in humans and mice. Hum Mol Genet. 2021;30(19):1881–93. https://doi.org/10.1093/hmg/ddab151.
2. Siewert A, Hoeland S, Mangold E, Ludwig KU. Combining genetic and single-cell expression data reveals cell types and novel candidate genes for orofacial clefting. Sci Rep. 2024;14(1):26492. https://doi.org/10.1038/s41598-024-77724-9.
3. Dixon MJ, Marazita ML, Beaty TH, Murray JC. Cleft lip and palate: understanding genetic and environmental influences. Nat Rev Genet. 2011;12(3):167–78. https://doi.org/10.1038/nrg2933.
4. Salari N, Darvishi N, Heydari M, Bokaee S, Darvishi F, Mohammadi M. Global prevalence of cleft palate, cleft lip and cleft palate and lip: a comprehensive systematic review and meta-analysis. J Stomatology Oral Maxillofacial Surg. 2022;123(2):110–20. https://doi.org/10.1016/j.jormas.
5. Zhou X, Jiang Y, Fang J, Wang H, Xie D, Kuang H, Li T, Liu Q, He J. Incidence of cleft lip and palate, and epidemiology of perinatal deaths related to cleft lip and palate in Hunan Province, China, 2016–2020. Sci Rep. 2023;13(1):10304. https://doi.org/10.1038/s41598-023-37436-y.
6. Fan D, Wu S, Liu L, Xia Q, Tian G, Wang W, Ye S, Wang L, Rao J, Yang X, Yu Z, Xin L, Li S, Duan Z, Zhang T, Wu S, Guo X, Liu Z. Prevalence of non-syndromic orofacial clefts: based on 15,094,978 Chinese perinatal infants. Oncotarget. 2018;9(17):13981–90. https://doi.org/10.18632/oncotarget.24238.
7. Sabbagh HJ, Baghlaf KK, Jamalellail HMH, Bakhuraybah AS, AlGhamdi SM, Alharbi OA, AlHarbi KM, Hassan MHA. Environmental tobacco smoke exposure and non-syndromic orofacial cleft: systematic review and meta-analysis. Tob Induc Dis. 2023;21:76. https://doi.org/10.18332/tid/163177.
8. Chevrier C, Bahuau M, Perret C, Iovannisci DM, Nelva A, Herman C, Vazquez MP, Francannet C, Robert-Gnansia E, Lammer EJ, Cordier S. Genetic susceptibilities in the association between maternal exposure to tobacco smoke and the risk of nonsyndromic oral cleft. Am J Med Genet. 2008;146A(18):2396–406. https://doi.org/10.1002/ajmg.a.32505.
9. Honein MA, Rasmussen SA, Reefhuis J, Romitti PA, Lammer EJ, Sun L, Correa A. Maternal smoking and environmental tobacco smoke exposure and the risk of orofacial clefts. Epidemiology. 2007;18(2):226–33. https://doi.org/10.1097/01.ede.0000254430.61294.c0.
10. Wu T, Liang KY, Hetmanski JB, Ruczinski I, Fallin MD, Ingersoll RG, Wang H, Huang S, Ye X, Wu-Chou YH, Chen PK, Jabs EW, Shi B, Redett R, Scott AF, Beaty TH. Evidence of gene-environment interaction for the IRF6 gene and maternal multivitamin supplementation in controlling the risk of cleft lip with/without cleft palate. Hum Genet. 2010;128(4):401–10. https://doi.org/10.1007/s00439-010-0863-y.
11. Bush JO, Jiang R. Palatogenesis: morphogenetic and molecular mechanisms of secondary palate development. Development. 2012;139(2):231–43. https://doi.org/10.1242/dev.067082.
12. Nasreddine G, El Hajj J, Ghassibe-Sabbagh M. Orofacial clefts embryology, classification, epidemiology, and genetics. Mutat Res Reviews Mutat Res. 2021;787:108373. https://doi.org/10.1016/j.mrrev.2021.108373.
13. Yu K, Deng M, Naluai-Cecchini T, Glass IA, Cox TC. Differences in oral structure and tissue interactions during mouse vs. human palatogenesis: implications for the translation of findings from mice. Front Physiol. 2017;8:154. https://doi.org/10.3389/fphys.2017.00154.
14. Hammond NL, Dixon MJ. Revisiting the embryogenesis of lip and palate development. Oral Dis. 2022;28(5):1306–26. https://doi.org/10.1111/odi.14174.
15. Lan Y, Xu J, Jiang R. Cellular and molecular mechanisms of palatogenesis. Curr Top Dev Biol. 2015;115:59–84. https://doi.org/10.1016/bs.ctdb.2015.07.002
16. Stanier P, Pauws E. Development of the lip and palate: FGF signalling. Front Oral Biol. 2012;16:71–80. https://doi.org/10.1159/000337618.
17. Babai A, Irving M. Orofacial clefts: genetics of cleft lip and palate. Genes (Basel). 2023;14(8):1603. https://doi.org/10.3390/genes14081603.

18. Park J, Ahn SH, Shin MG, Kim HK, Chang S. TRNA-derived small RNAs: novel epigenetic regulators. Cancers (Basel). 2020;12(10):2773. https://doi.org/10.3390/cancers12102773.
19. Dhahbi JM, Spindler SR, Atamna H, Boffelli D, Martin DI. Deep sequencing of serum small RNAs identifies patterns of 5′ tRNA half and YRNA fragment expression associated with breast cancer. Biomark Cancer. 2014;6:37–47. https://doi.org/10.4137/BIC.S20764.
20. Oberbauer V, Schaefer MR. TRNA-derived small RNAs: Biogenesis, modification, function and potential impact on human disease development. Genes (Basel). 2018;9(12):607. https://doi.org/10.3390/genes9120607.
21. Zhu L, Li J, Gong Y, Wu Q, Tan S, Sun D, Xu X, Zuo Y, Zhao Y, Wei YQ, Wei XW, Peng Y. Exosomal tRNA-derived small RNA as a promising biomarker for cancer diagnosis. Mol Cancer. 2019;18(1):74. https://doi.org/10.1186/s12943-019-1000-8.
22. Kumar P, Kuscu C, Dutta A. Biogenesis and function of transfer RNA-related fragments (tRFs). Trends Biochem Sci. 2016;41(8):679–89. https://doi.org/10.1016/j.tibs.2016.05.004.
23. Xiong Q, Zhang Y, Xu Y, Yang Y, Zhang Z, Zhou Y, Zhang S, Zhou L, Wan X, Yang X, Zeng Z, Liu J, Zheng Y, Han J, Zhu Q. tiRNA-Val-CAC-2 interacts with FUBP1 to promote pancreatic cancer metastasis by activating cMYC transcription. Oncogene. 2024;43(17):1274–87. https://doi.org/10.1038/s41388-024-02991-9.
24. Chen Y, Shao Z, Wu S. Research progress on the tsRNA biogenesis, function, and application in lung cancer. Non-coding RNA Res. 2024;10:63–9. https://doi.org/10.1016/j.ncrna.2024.09.004.
25. Li Y, Yu Z, Jiang W, Lyu X, Guo A, Sun X, Yang Y, Zhang Y. tRNA and tsRNA: from heterogeneity to multifaceted regulators. Biomolecules. 2024;14(10):1340. https://doi.org/10.3390/biom14101340.
26. Selitsky SR, Baran-Gale J, Honda M, Yamane D, Masaki T, Fannin EE, Guerra B, Shirasaki T, Shimakami T, Kaneko S, Lanford RE, Lemon SM, Sethupathy P. Small tRNA-derived RNAs are increased and more abundant than microRNAs in chronic hepatitis B and C. Sci Rep. 2015;5:7675. https://doi.org/10.1038/srep07675.
27. Sun C, Yang F, Zhang Y, Chu J, Wang J, Wang Y, Zhang Y, Li J, Li Y, Fan R, Li W, Huang X, Wu H, Fu Z, Jiang Z, Yin Y. TRNA-derived fragments as novel predictive biomarkers for trastuzumab-resistant breast cancer. Cell Physiol Biochem. 2018;49(2):419–31. https://doi.org/10.1159/000492977.
28. Li P, Tang T, Liu T, Zhou J, Cui H, He Z, Zhong Y, Hu E, Yang A, Wei G, Luo J, Wang Y. Systematic analysis of tRNA-derived small RNAs reveals novel potential therapeutic targets of traditional Chinese medicine (Buyang-Huanwu-Decoction) on intracerebral hemorrhage. Int J Biol Sci. 2019;15(4):895–908. https://doi.org/10.7150/ijbs.29744.
29. Chen Q, Yan M, Cao Z, Li X, Zhang Y, Shi J, Feng GH, Peng H, Zhang X, Zhang Y, Qian J, Duan E, Zhai Q, Zhou Q. Sperm tsRNAs contribute to intergenerational inheritance of an acquired metabolic disorder. Science. 2016;351(6271):397–400. https://doi.org/10.1126/science.aad7977.
30. Bak ST, Haupt-Jorgensen M, Dudele A, Wegener G, Wang T, Nielsen AL, Lund S. The anti-inflammatory agent 5-ASA reduces the level of specific tsRNAs in sperm cells of high-fat fed C57BL/6J mouse sires and improves glucose tolerance in female offspring. J Diabetes Complicat. 2023;37(9):108563. https://doi.org/10.1016/j.jdiacomp.2023.108563.
31. Victor Veau. Division palatine, anatomie, chirurgie, phonétique. J Am Med Association Paris: Masson. 1931;99(12):1017–8.
32. Lu C, Wang JY, Jia ZL. Environmental factors of non-syndromic cleft lip and palate. Hua Xi Kou Qiang Yi Xue Za Zhi. 2019;37(5):547–50. https://doi.org/10.7518/hxkq.2019.05.018.
33. Kerpedjiev P, Hammer S, Hofacker IL. Forna (force-directed RNA): simple and effective online RNA secondary structure diagrams. Bioinformatics. 2015;31(20):3377–9. https://doi.org/10.1093/bioinformatics/btv372.
34. Bruccoleri RE, Heinrich G. An improved algorithm for nucleic acid secondary structure display. Comput Appl Biosci. 1988;4(1):167–73. https://doi.org/10.1093/bioinformatics/4.1.167.
35. Kim HK, Xu J, Chu K, Park H, Jang H, Li P, Valdmanis PN, Zhang QC, Kay MA. A tRNA-derived small RNA regulates ribosomal protein S28 protein levels after translation initiation in humans and mice. Cell Rep. 2019;29(12):3816–24. https://doi.org/10.1016/j.celrep.2019.11.062.
36. Jensen BL, Kreiborg S, Dahl E, Fogh-Andersen P. Cleft lip and palate in Denmark, 1976–1981: epidemiology, variability, and early somatic development. Cleft Palate J. 1988;25(3):258–69.
37. van Aalst JA, Kolappa KK, Sadove M. MOC-PSSM CME article: nonsyndromic cleft palate. Plast Reconstr Surg. 2008;121(1 Suppl):1–14. https://doi.org/10.1097/01.prs.0000294706.05898.f3.
38. Yoshida N, Inubushi T, Hirose T, Aoyama G, Kurosaka H, Yamashiro T. The roles of JAK2/STAT3 signaling in fusion of the secondary palate. Dis Models Mech. 2023;16(10):dmm050085. https://doi.org/10.1242/dmm.050085.
39. Richardson RJ, Hammond NL, Coulombe PA, Saloranta C, Nousiainen HO, Salonen R, Berry A, Hanley N, Headon D, Karikoski R, Dixon MJ. Periderm prevents pathological epithelial adhesions during embryogenesis. J Clin Investig. 2014;124(9):3891–900. https://doi.org/10.1172/JCI71946.
40. Ye F, Xu H, Yin H, Zhao X, Li D, Zhu Q, Wang Y. The role of BMP6 in the proliferation and differentiation of chicken cartilage cells. PLoS ONE. 2019;14(7):e0204384. https://doi.org/10.1371/journal.pone.0204384.
41. Liu X, Li Z, Song Y, Wang R, Han L, Wang Q, Jiang K, Kang C, Zhang Q. AURKA induces EMT by regulating histone modification through Wnt/β-catenin and PI3K/Akt signaling pathway in gastric cancer. Oncotarget. 2016;7(22):33152–64. https://doi.org/10.18632/oncotarget.8888.
42. Xie Y, Yao L, Yu X, Ruan Y, Li Z, Guo J. Action mechanisms and research methods of tRNA-derived small RNAs. Signal Transduct Target Therapy. 2020;5(1):109. https://doi.org/10.1038/s41392-020-00217-4.
43. Karaiskos S, Naqvi AS, Swanson KE, Grigoriev A. Age-driven modulation of tRNA-derived fragments in Drosophila and their potential targets. Biol Direct. 2015;10:51. https://doi.org/10.1186/s13062-015-0081-6.
44. Komiyama Y, Koshiji C, Yoshida W, Natsume N, Kawamata H. 5,10-Methylenetetrahydrofolate reductase (MTHFR) C677T/A1298C polymorphisms in patients with nonsyndromic cleft lip and palate. Biomedical Rep. 2020;13(6):57. https://doi.org/10.3892/br.2020.1364.
45. Bufalino A, Ribeiro Paranaíba LM, Nascimento de Aquino S, Martelli-Júnior H, Oliveira Swerts MS, Coletta RD. Maternal polymorphisms in folic acid metabolic genes are associated with nonsyndromic cleft lip and/or palate in the Brazilian population. Birth Defects Res a. 2010;88(11):980–6. https://doi.org/10.1002/bdra.20732.
46. Longo N. Disorders of biopterin metabolism. J Inherit Metabolic Dis. 2009;32(3):333–42. 10.1007/ s10545-009-1067-2.
47. Wu Y, Chen P, Sun L, Yuan S, Cheng Z, Lu L, Du H, Zhan M. Sepiapterin reductase: characteristics and role in diseases. J Cell Mol Med. 2020;24(17):9495–506. https://doi.org/10.1111/jcmm.15608.
48. Werner ER, Blau N, Thöny B. Tetrahydrobiopterin: biochemistry and pathophysiology. Biochem J. 2011;438(3):397–414. https://doi.org/10.1042/BJ20110293.
49. Xu F, Sudo Y, Sanechika S, et al. Disturbed biopterin and folate metabolism in the Qdpr-deficient mouse. FEBS Lett. 2014;588(21):3924–31. https://doi.org/10.1016/j.febslet.2014.09.004.
50. Feldman RM, Correll CC, Kaplan KB, Deshaies RJ. A complex of Cdc4p, Skp1p, and Cdc53p/cullin catalyzes ubiquitination of the phosphorylated CDK inhibitor Sic1p. Cell. 1997;91(2):221–30. https://doi.org/10.1016/s0092-8674(00)80404-3.
51. Zheng N, Shabek N. Ubiquitin ligases: structure, function, and regulation. Annu Rev Biochem. 2017;86:129–57. https://doi.org/10.1146/annurev-biochem-060815-014922.
52. Su J, Li M, Chang Y, Jia M, Zhao M, Guan S, Niu J, Zhang S, Yang H, Sun M. Discovery of the 2,4-disubstituted quinazoline derivative as a novel neddylation inhibitor for tumor therapy. Bioorg Chem. 2024;145:107237. https://doi.org/10.1016/j.bioorg.2024.107237.
53. Jin J, Cardozo T, Lovering RC, Elledge SJ, Pagano M, Harper JW. Systematic analysis and nomenclature of mammalian F-box proteins. Genes Dev. 2004;18(21):2573–80. https://doi.org/10.1101/gad.1255304.
54. Skowyra D, Craig KL, Tyers M, Elledge SJ, Harper JW. F-box proteins are receptors that recruit phosphorylated substrates to the SCF ubiquitin-ligase complex. Cell. 1997;91(2):209–19. https://doi.org/10.1016/s0092-8674(00)80403-1.
55. Francis-West PH, Tatla T, Brickell PM. Expression patterns of the bone morphogenetic protein genes BMP4 and BMP2 in the developing chick face suggest a role in outgrowth of the primordia. Dev Dynamics: Official Publication Am Association Anatomists. 1994;201(2):168–78. https://doi.org/10.1002/aja.1002010207
56. García Muro AM, García Ruvalcaba A, Rizo de la Torre LDC, Sánchez López JY. Role of the BMP6 protein in breast cancer and other types of cancer. Growth Factors. 2021;39(1–6):1–13. https://doi.org/10.1080/08977194.2021.1994964.

57. Zhang Y, Murugesan P, Huang K, Cai H. NADPH oxidases and oxidase crosstalk in cardiovascular diseases: novel therapeutic targets. Nat Rev Cardiol. 2020;17(3):170–94. https://doi.org/10.1038/s41569-019-0260-8.